Heredity (2017) 119, 125–135

www.nature.com/hdy

ORIGINAL ARTICLE

Genetic-based interactions among tree neighbors: identification of the most influential neighbors, and estimation of correlations among direct and indirect genetic effects for leaf disease and growth in *Eucalyptus globulus*

J Costa e Silva[1], BM Potts[2], AR Gilmour[3] and RJ Kerr[4]

An individual's genes may influence the phenotype of neighboring conspecifics. Such indirect genetic effects (IGEs) are important as they can affect the apparent total heritable variance in a population, and thus the response to selection. We studied these effects in a large, pedigreed population of *Eucalyptus globulus* using variance component analyses of Mycosphearella leaf disease, diameter growth at age 2 years, and post-infection diameter growth at ages 4 and 8 years. In a novel approach, we initially modeled IGEs using a factor analytic (FA) structure to identify the most influential neighbor positions, with the FA loadings being position-specific regressions on the IGEs. This involved sequentially comparing FA models for the variance–covariance matrices of the direct and indirect effects of each neighbor. We then modeled IGEs as a distance-based, combined effect of the most influential neighbors. This often increased the magnitude and significance of indirect genetic variance estimates relative to using all neighbors. The extension of a univariate IGEs model to bivariate analyses also provided insights into the genetic architecture of this population, revealing that: (1) IGEs arising from increased probability of neighbor infection were not associated with reduced growth of neighbors, despite adverse fitness effects being evident at the direct genetic level; and (2) the strong, genetic-based competitive interactions for growth, established early in stand development, were highly positively correlated over time. Our results highlight the complexities of genetic-based interactions at the multi-trait level due to (co)variances associated with IGEs, and the marked discrepancy occurring between direct and total heritable variances.
Heredity (2017) **119,** 125–135; doi:10.1038/hdy.2017.25; published online 31 May 2017

INTRODUCTION

Recent developments in quantitative genetics suggest that interactions among conspecifics may change the understanding of the inheritance and response to selection for polygenic traits (Bijma, 2011). Classical quantitative genetic models have overlooked the fact that an individual's genes may also influence the phenotype of neighboring conspecifics. Such indirect genetic effects (IGEs; Griffing, 1967; Moore *et al.*, 1997; Wolf *et al.*, 1998; Bijma, 2014) may occur by, for example, competitive interactions (Muir, 2005; Bijma *et al.*, 2007; Muir *et al.*, 2013; Wilson, 2014), as well as exposure to disease infection (Lipschutz-Powell *et al.*, 2012; Anche *et al.*, 2014), with both recently reported among trees in a plantation (Costa e Silva *et al.*, 2013). As with direct genetic effects, IGEs are dynamic and may change with age (Moorad and Nussey, 2016), sex (Wilson *et al.*, 2011) and environment (Camerlink *et al.*, 2015), and they may arise from multiple genetic causes (Wolf *et al.*, 2011; Bailey and Hoskins, 2014). IGEs underlie many 'social' interactions in plants and animals (Bijma, 2014; Wilson, 2014), may vary across a species range (Bailey *et al.*, 2014) and, at the interspecific level (IIGEs), structure biological communities (Shuster *et al.*, 2006).

Within a univariate variance-component framework, a quantitative genetic model including IGEs seeks to estimate the covariance between direct and indirect genetic effects. This is a key determinant of the impact of indirect genetic effects on the heritable variation available at the population level for a trait affected by interactions among conspecifics (Griffing, 1967; Bijma *et al.*, 2007; Bijma, 2011). However, as selection operates on complex phenotypes involving several correlated traits, it is important to also consider covariances among traits for direct and indirect genetic effects to better understand and predict genetic responses to selection (McGlothlin *et al.*, 2010). Under either a variance-component or a trait-based modeling of IGEs (McGlothlin and Brodie, 2009; Bijma, 2014), recent studies have used multivariate approaches to address direct and indirect genetic relationships among traits in animals (for example, Peeters *et al.*, 2012; Bailey and Hoskins, 2014) and in plants (for example, Mutic and Wolf, 2007; Wolf *et al.*, 2011) but, to our knowledge, no such multivariate studies have yet been reported in forest trees.

Previous univariate models evaluating the genetic basis of interactions among trees have assumed that the indirect breeding values of all the surviving immediate neighbors impacted on the focal individual's

[1]Centro de Estudos Florestais, Instituto Superior de Agronomia, Universidade de Lisboa, Lisboa, Portugal; [2]School of Biological Sciences and ARC Training Centre for Forest Value, University of Tasmania, Hobart, Tasmania, Australia; [3]11 Holman Way, Orange, New South Wales, Australia and [4]PlantPlan Genetics Pty Ltd., c/o School of Biological Sciences, University of Tasmania, Hobart, Tasmania, Australia
Correspondence: Dr J Costa e Silva, Centro de Estudos Florestais, Instituto Superior de Agronomia, Universidade de Lisboa, Tapada da Ajuda, Lisboa 1349-017, Portugal.
E-mail: jces@isa.ulisboa.pt
Received 15 November 2016; revised 10 March 2017; accepted 9 April 2017; published online 31 May 2017

phenotype (Cappa and Cantet, 2008; Costa e Silva and Kerr, 2013; Costa e Silva *et al.*, 2013; Cappa *et al.*, 2015). They devised weights based on distance to each neighbor to integrate the neighbor effects into a modeling of IGEs as a combined effect. However, it begs the question whether the weights are optimal, and whether cardinal direction or cultural operations may moderate the position effect. For example, the neighbor effect could be moderated by prevailing wind direction, by slope and aspect and dominant direction of sunlight. In forest genetic trials, identifying the neighbor positions contributing most to IGEs is important because: (1) it may enable better detection of IGEs under a variance-component framework; and (2) it has implications for the accurate estimation of the total heritable variance determining potential response to selection.

Using a large pedigreed population of the forest tree *Eucalyptus globulus*, the present study aims to:

- develop an approach to identify the neighbor positions contributing most to IGEs for Mycosphearella leaf disease and diameter growth;
- follow over time the estimates of direct and indirect additive genetic (co)variance parameters and total heritable variance obtained for diameter growth; and
- extend univariate models to the multivariate level to assess the magnitude and significance of correlations among direct and/or indirect additive genetic effects between traits (leaf disease and post-infection growth) and ages.

MATERIALS AND METHODS

Plant material, crossing design, field experiment and trait measurements

The plant material was generated by combining crosses from both diallel and factorial mating schemes, and evaluated in a field trial located in Western Australia (latitude 34°13′34″ S, longitude 116°8′37″ E). Both mating schemes were unbalanced. A total of 570 full-sib families were planted, generated from 51 parents in the diallel crosses and 110 parents in the factorial crosses. The diallel scheme incorporated reciprocal mating but no self crosses. The factorial crosses were included to provide genetic links with previous breeding and research trials. The *E. globulus* trees used as parents in the crosses were in general selected from first-generation breeding trials, with the base population parents belonging to three races (Furneaux, Strzelecki Ranges and Otways; for Otways, all are from the Western Otways except one which was from the proximal Eastern Otways) and eight races (Furneaux, King Island, North- and South-eastern Tasmania, Southern Tasmania, Strzelecki Ranges, Eastern and Western Otways) for the diallel and factorial schemes, respectively. The numbers of parents and crosses in the diallel differed slightly from those reported by Costa e Silva *et al.* (2013), as some parents were re-allocated to the factorial to improve the number of families per parent and geographic focus of the parents in the diallel. The base population parents were assumed to be unrelated and non-inbred due to widely spaced sampling.

The field experiment was designed as a resolvable row–column design (John and Williams, 1995) with 15 replicates. One seedling per full-sib family was randomly planted as a single-tree plot within each replicate, and the tree spacing was 2.125 and 5.0 m within and between planting rows, respectively. There were 9450 trees originally planted in an incomplete rectangular grid of 72 rows by 161 columns. For spatial modeling purposes (see below), coordinates with missing values were added to complete the planting grid, which is a standard practice in spatial analysis of field trials with an irregular shape (Gilmour *et al.*, 2015).

There was an outbreak of Mycosphaerella leaf disease (MLD) 2 years after planting. Each tree was then assessed for the percentage of the juvenile foliage affected by MLD, following the method described by Milgate *et al.* (2005). Over-bark diameter at breast height (DBH) was measured at 2, 4 and 8 years from planting, with the later age corresponding to about half the harvest age of *E. globulus* plantations. The MLD mean was 23% (s.d. = 11%), and the DBH means increased from 98 mm (s.d. = 16 mm) at age 2 to 175 mm (s.d. = 37 mm) at age 8 years. The mean tree survival was high, dropping from 96% at age 2 to 93% at age 8 years.

The sequence and rationale of the analytic steps followed to model our data are depicted in Figure 1, and further details are given below and in Supplementary Information.

Univariate data analysis

Definition of the general statistical model. For each trait at a given age, the following univariate general linear mixed model was fitted:

$$\mathbf{y} = \mathbf{Xb} + \mathbf{Z}_a\mathbf{u}_a + \mathbf{Z}_s\mathbf{u}_s + \mathbf{Z}_m\mathbf{u}_m + \mathbf{Z}_r\mathbf{u}_r + \mathbf{Z}_o\mathbf{u}_o + \mathbf{e} \quad (1)$$

where $\mathbf{y}$ is a vector of individual tree observations, $\mathbf{b}$ is a vector of fixed effects, $\mathbf{u}_a$ is a vector of random additive genetic effects, $\mathbf{u}_s$ is a vector of random full-sib family effects, $\mathbf{u}_m$ is a vector of random maternal effects in the diallel, $\mathbf{u}_r$ is a vector of random reciprocal effects in the diallel, $\mathbf{u}_o$ is a vector of additional random effects, $\mathbf{e}$ is a vector of random residual effects and $\mathbf{X}$, $\mathbf{Z}_a$, $\mathbf{Z}_s$, $\mathbf{Z}_m$, $\mathbf{Z}_r$ and $\mathbf{Z}_o$ are incidence matrices linking a tree's phenotype to the fixed and random effects. The vector $\mathbf{b}$ included the overall trait mean and a term to account for the race effects within each cross type (that is, diallel or factorial). The vector $\mathbf{u}_a$ was composed of sub-vectors comprising direct and indirect additive genetic effects. The vector $\mathbf{u}_s$ contained full-sib family effects for each cross type. The vector $\mathbf{u}_o$ included effects for the different experimental design features such as replicates, and rows and columns within replicates. The residual term $\mathbf{e}$ was partitioned into $\mathbf{e} = \boldsymbol{\xi} + \boldsymbol{\eta}$, with the elements in vector $\boldsymbol{\xi}$ following a spatial autoregressive process and the elements in vector $\boldsymbol{\eta}$ being distributed independently of each other and of those in $\boldsymbol{\xi}$. Vectors $\mathbf{b}$ and $\mathbf{u}_o$ also included terms to remove non-stationarity from $\boldsymbol{\xi}$.

Under the general mixed model specified in Equation (1), the joint distribution of the random terms was assumed to be multivariate normal with a zero-mean vector and a block-diagonal variance matrix, specified as a direct sum of variance–covariance matrices related to the effects in $\mathbf{u}_a$, $\mathbf{u}_s$, $\mathbf{u}_m$, $\mathbf{u}_r$, $\mathbf{u}_o$ and $\mathbf{e}$. The form of the variance–covariance matrices for effects in $\mathbf{u}_o$ and $\mathbf{e}$ depended on the analysis that was carried out for modeling the interactions between a focal tree and its immediate neighbors, as described below. An arcsine transformation (that is, $\sin^{-1}(\sqrt{\text{MLD}})$) was applied for the MLD data, as preliminary analysis of this trait indicated that the distribution of the model residuals was slightly skewed.

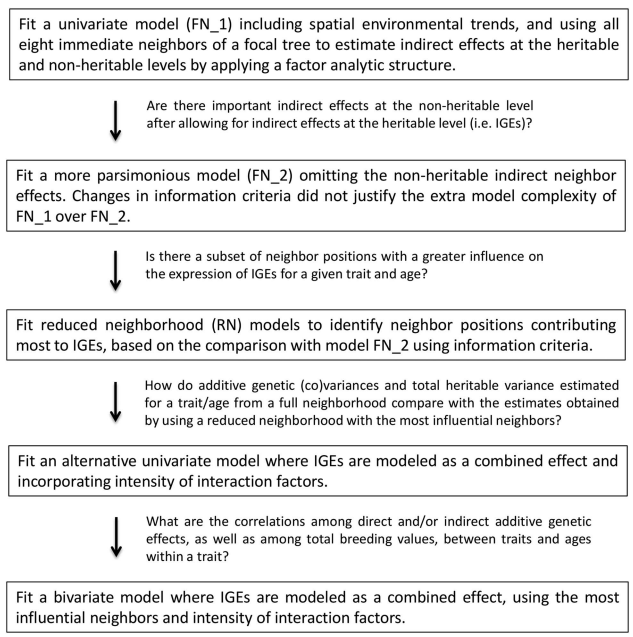

Figure 1 Sequence of analyses followed to model indirect effects at the heritable and non-heritable levels for the MLD and DBH data measured in a forest genetic trial of *Eucalyptus globulus*.

Modeling individual neighbor effects. In forest genetic trials, trees are usually planted in a rectangular or square grid indexed by row and column numbers, and so a focal tree has up to eight immediate neighbors (Figure 2). We jointly modeled the covariance of a focal tree with its eight immediate neighbors with the aim of identifying the positions impacting most on IGEs. For this purpose, we considered three basic models as follows:

- indirect effects at both the heritable (that is, additive genetic) and non-heritable (that is, independent residual) levels, using all eight neighbors (hereafter called model FN_1);
- indirect effects at the additive genetic level only, using all eight neighbors (hereafter called model FN_2); and
- indirect effects at the additive genetic level only, using a subset of the neighbor positions (hereafter called model RN).

In models FN_1 and FN_2, $\mathbf{u}_a = \left(\mathbf{u}'_{a_d}, \mathbf{u}'_{a_{i(K_1)}}, \mathbf{u}'_{a_{i(K_2)}}, ..., \mathbf{u}'_{a_{i(K_8)}}\right)'$ with the related incidence matrix given by $\mathbf{Z}_a = \left(\mathbf{Z}_{a_d}, \mathbf{Z}_{a_{i(K_1)}}, \mathbf{Z}_{a_{i(K_2)}}, ..., \mathbf{Z}_{a_{i(K_8)}}\right)$, where the subscripts d and i denote direct and indirect effects, respectively, the subscripts K_1 to K_8 denote the neighbor positions (Figure 2), and the superscript $'$ refers to the transpose operation. $\mathbf{Z}_{a_d}$ relates the phenotype of a focal tree to its own direct additive genetic effect, and $\mathbf{Z}_{a_{i(K_1)}}$ to $\mathbf{Z}_{a_{i(K_8)}}$ relate the phenotype of a focal tree to the indirect additive genetic effect of each of its eight immediate neighbors (that is, from K_1 to K_8). For the indirect genetic effects under model RN, $\mathbf{u}_a$ and $\mathbf{Z}_a$ pertained to a reduced set of neighbors. To model the IGEs as a common effect across positions except for scale, we used a constrained factor analytic structure with one factor, hereafter denoted as FA1, for the genetic effects in $\mathbf{u}_a$. A common indirect effect was modeled by setting the specific variances (representing variation that is not explained by the factor) associated with the neighbor effects to zero, so that the correlations between the indirect effects of K_1 to K_8 and the direct effect are the same except for sign, and the correlations among the indirect effects of K_1 to K_8 are all one or minus one. Thus, the 'factor' represents the common indirect effect, and the loading for a given neighbor represents the size (scale) of the effect in that direction. This constrained FA1 matrix with 10 parameters was used in models FN_1 and FN_2. A reduced form, obtained by deleting certain neighbor positions, was used in model RN. Further details on modeling effects in $\mathbf{u}_a$ are given in Supplementary Note S1 (Supplementary Information).

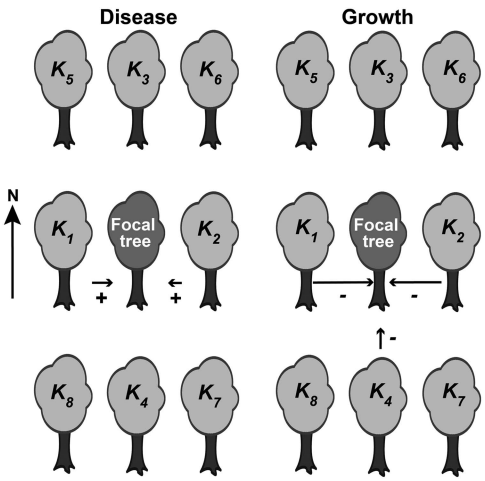

Figure 2 Neighborhood consisting of a focal tree and its eight immediate neighbors, and the neighbors contributing most to IGEs for Mycosphearella leaf disease (MLD) and breast-height stem diameter (DBH) growth at ages 2 and 4 years, respectively. The same-row neighbors are denoted as K_1 and K_2; the same-column neighbors are denoted as K_3 and K_4; and the diagonal neighbors are denoted as K_5, K_6, K_7 and K_8. The inter-column (within row) spacing corresponds to a distance between the focal tree and K_1 or K_2 of 2.125 m, and the inter-row spacing corresponds to a distance between the focal tree and K_3 or K_4 of 5 m. The direction to the north is also depicted. The arrows indicate the neighbors contributing most to IGEs, as detected when modeling IGEs as individual neighbor effects by using a factor analytic structure with one factor (FA1). In this context, the arrow length is proportional to the parameter estimate/standard error ratio of a neighbor's loading on the common factor, standardized by the maximum value observed for this ratio across the two illustrated cases. The sign of the direct–indirect genetic covariance between the focal tree and each of its influential neighbors is also shown. The FA1 model for MLD had a generally positive correlation between direct and indirect genetic effects, which reflects the infection process; the FA1 model for DBH had a generally negative correlation between direct and indirect genetic effects, reflecting competitive interactions (see Supplementary Table S1 and its footnotes for further details).

In these three models, the spatially correlated residuals in $\boldsymbol{\xi}$ were modeled by a variance–covariance structure based on a separable autoregressive process in the row and column directions of the field layout, and thus $Var(\boldsymbol{\xi}) = \sigma^2_{ce}[\boldsymbol{\Sigma}_{row}(\phi_{row}) \otimes \boldsymbol{\Sigma}_{col}(\phi_{col})]$, where σ^2_{ce} is the variance of the trend (correlated residual) process, and $\boldsymbol{\Sigma}_{row}$ and $\boldsymbol{\Sigma}_{col}$ are autoregressive correlation matrices with autocorrelation parameters ϕ_{row} and ϕ_{col} for row and column directions, respectively. In addition, under model FN_1, we explicitly modeled direct and indirect (co)variances pertaining to non-heritable effects that may cause interactions between a focal tree and its immediate neighbors, and distributed independently of the correlated residuals in $\boldsymbol{\xi}$. In this sense, and akin to effects in $\mathbf{u}_a$, we used a FA1 structure to model the variance–covariance matrix for the independent residuals in $\boldsymbol{\eta}$. For models FN_2 and RN, the residuals in $\boldsymbol{\eta}$ were assumed to represent direct non-heritable effects only. Further details on the modeling of effects in $\boldsymbol{\xi}$ and $\boldsymbol{\eta}$ are provided in Supplementary Note S2 (Supplementary Information).

We used the Akaike's (AIC; Akaike, 1974) and Schwarz's Bayesian (BIC; Schwarz, 1978) information criteria (see Supplementary Note S3 in Supplementary Information) to successively compare the models. The comparison of model FN_2 to model FN_1 assessed whether there was important non-heritable indirect effects after allowing for indirect effects at the genetic level. Then, assuming that FN_2 was a plausible model, several RN models were compared to the model FN_2 to assess whether all eight neighbor positions were necessary for modeling IGEs. Differences (Δ) in AIC or BIC values were computed with respect to the more parsimonious model (that is, FN_2 and RN in the first and second comparisons described above, respectively). Supplementary Note S4 (Supplementary Information) describes the procedure used to compare RN and FN_2 models for identifying those neighbor positions with the greatest influence on the expression of IGEs for a given trait and age.

Modeling a combined indirect effect. The preceding models used a FA1 structure to define an underlying factor for indirect effects, and the loadings provided the regression or weighting of this factor with respect to the various neighbor positions. Thus, the underlying factor in the FA1 model represents a common indirect effect. Alternatively, one can calculate a combined indirect effect using a sum of weighted neighbor design matrices, where the weights are calculated as 'intensity of interaction factors' based on neighbor distance, as done by earlier authors (for example, Cappa and Cantet, 2008; Costa e Silva and Kerr, 2013). In the present case, we used both approaches in a complementary manner, by first applying the FA1 structure to identify the neighbor positions contributing most to IGEs, and then using these influential neighbors to model a combined indirect effect (Figure 1). Supplementary Note S5 (Supplementary Information) describes the methodological details in regard to the modeling of a combined indirect effect under univariate data analysis.

Bivariate data analysis

To study the genetic relationships between pairs of traits or ages, we extended the univariate approach that modeled IGEs as a combined effect using the most influential neighbors and intensity of interaction factors to obtain a bivariate linear mixed model which, following a reformulation of Equation (1), can be

represented as:

$$\mathbf{y} = \mathbf{Xb} + \mathbf{Z}_{a_d}\mathbf{u}_{a_d} + \mathbf{Z}_{a_i}\mathbf{u}_{a_i} + \sum_{l=1}^{t}\mathbf{Z}_l\mathbf{u}_l + \boldsymbol{\xi} + \boldsymbol{\eta} \quad (2)$$

where $\mathbf{y} = (\mathbf{y}_1', \mathbf{y}_2')'$, $\mathbf{X} = diag(\mathbf{X}_1, \mathbf{X}_2)$, $\mathbf{b} = (\mathbf{b}_1', \mathbf{b}_2')'$, $\mathbf{Z}_{a_d} = diag(\mathbf{Z}_{a_{d_1}}, \mathbf{Z}_{a_{d_2}})$, $\mathbf{u}_{a_d} = (\mathbf{u}_{a_{d_1}}', \mathbf{u}_{a_{d_2}}')'$, $\mathbf{Z}_{a_i} = diag(\mathbf{Z}_{a_{i_1}}, \mathbf{Z}_{a_{i_2}})$, $\mathbf{u}_{a_i} = (\mathbf{u}_{a_{i_1}}', \mathbf{u}_{a_{i_2}}')'$, $\mathbf{Z}_l = diag(\mathbf{Z}_{l_1}, \mathbf{Z}_{l_2})$, $\mathbf{u}_l = (\mathbf{u}_{l_1}', \mathbf{u}_{l_2}')'$, $\boldsymbol{\xi} = (\boldsymbol{\xi}_1', \boldsymbol{\xi}_2')'$ and $\boldsymbol{\eta} = (\boldsymbol{\eta}_1', \boldsymbol{\eta}_2')'$; $\sum_{l=1}^{t}\mathbf{Z}_l\mathbf{u}_l$ includes each of the terms defined under Equation (1) for full-sib family, maternal, reciprocal and additional random effects; the subscripts 1 and 2 refer to a pair of traits or ages.

The vector **b** included a mean term, as well as other fixed effects fitted as required for each trait or age. For all the random terms defined under Equation (2), the description of the corresponding variance–covariance matrices is provided in Supplementary Note S6 (Supplementary Information).

Parameter estimation

Restricted maximum likelihood (REML) estimates of (co)variance parameters were obtained by using the Average Information REML algorithm developed by Gilmour *et al.* (1995), and implemented in the ASReml software (Gilmour *et al.*, 2015). The phenotypic variance for a trait at a given age was calculated as described by Costa e Silva *et al.* (2013). On the basis of the REML estimates of additive genetic (co)variances obtained by modeling IGEs as a combined effect, direct–indirect genetic correlations were calculated for a trait at a given age under the univariate analysis, and between traits or ages under the bivariate analysis. In addition, the correlation between the total breeding values of two traits or ages ($r_{TBV_{(1,2)}}$) was computed as described in Supplementary Note S7 (Supplementary Information).

Taylor series expansion was used to obtain approximate standard errors for the (co)variance parameters estimated from the linear mixed model, as well as for derived linear combinations or ratios of the (co)variance estimates (Lynch and Walsh, 1998; Gilmour *et al.*, 2015). Because of the computational time required to fit more complex models, no attempts were made to formally test the significance of the genetic correlations estimated under the bivariate analysis, although REML likelihood-ratio tests were used to test the significance of (co)variance parameters estimated under simpler (univariate) models fitted for a given trait and age. Consequently, where adequate, the significance of a genetic correlation (that is, deviation from zero) was judged by a conservative approach based on the ratio of the parameter estimate relative to its approximate standard error (that is, a statistically significant outcome at the 5% level occurs when the ratio is $\geqslant 1.96$, assuming that it is asymptotically normally distributed).

RESULTS

Univariate data analysis

Modeling individual neighbor effects. Table 1 presents the results obtained from comparing model FN_2 to FN_1, and model RN to FN_2, by using the AIC and BIC information criteria. In general, the AIC and BIC tended to agree on the preferred model, although the magnitude of the differences in ΔAIC were considerably smaller than those in ΔBIC, reflecting the larger weight placed on the penalty for model complexity in the BIC relative to AIC (see Supplementary Note S3).

As a model for these data, FN_2 provided in general a better compromise between model fit and complexity than FN_1. For DBH, the negative values of $\Delta AIC_{(FN\_2,\ FN\_1)}$ and $\Delta BIC_{(FN\_2,\ FN\_1)}$ indicated that both information criteria preferred FN_2 over FN_1. For MLD, model FN_2 was clearly supported by the BIC only. However, despite its positive value (which would favor model FN_1), the magnitude of $\Delta AIC_{(FN\_2,\ FN\_1)}$ for MLD was $\leqslant 2$ which, according to the guidelines proposed by Burnham and Anderson (2002; page 70), indicates a substantial level of empirical support for FN_2. Hence, based on the AIC, model FN_2 was essentially as good as FN_1 for MLD, as the increase in REML log-likelihood obtained from FN_1 did not justify

Table 1 Modeling indirect effects at the non-heritable (that is, independent residual) and/or heritable (that is, additive genetic) levels as individual neighbor effects on a focal tree: model comparison using the AIC and BIC information criteria[a,b,c,d,e]

Trait (age)	*FN_1*		*FN_2*		*RN*		*Comparing FN_2 to FN_1*		*Comparing RN to FN_2*		*Neighbors kept in RN*	
	AIC	*BIC*	*AIC*	*BIC*	*AIC*	*BIC*	$\Delta AIC_{(FN\_2,\ FN\_1)}$	$\Delta BIC_{(FN\_2,\ FN\_1)}$	$\Delta AIC_{(RN,\ FN\_2)}$	$\Delta BIC_{(RN,\ FN\_2)}$	*Using AIC*	*Using BIC*
MLD (2 years)	55265.3	55471.6	55266.8	55409.1	55264.7	55364.3	1.5	−62.5	−2.1	−44.8	K_1, K_2	K_1, K_2
DBH (2 years)	57772.9	57972.1	57769.2	57911.5	57764.4	57864.0	−3.7	−60.6	−4.8	−47.5	K_1, K_2	K_1, K_2
DBH (4 years)	63371.0	63569.6	63368.4	63510.3	63367.5	63437.9	−2.6	−59.3	−0.9	−72.4	K_1, K_2, K_4	K_1, K_2, K_4
DBH (8 years)	70238.6	70443.8	70235.2	70376.8	70236.4	70342.5	−3.4	−67.0	1.2	−34.3	K_1, K_2, K_4	K_1, K_2, K_4

Abbreviations: AIC and BIC refer to the Akaike's (1974) and Schwarz's (1978) information criteria, respectively; FN and RN represent full and reduced neighborhoods, respectively; DBH and MLD denote stem diameter at breast-height and Mycosphaerella leaf disease, respectively.
[a]The models compared correspond to: FN_1, modeling indirect effects at both the heritable and non-heritable levels, using all eight immediate neighbors of a focal tree; FN_2, modeling indirect effects at the heritable level only, using all eight immediate neighbors of a focal tree; and RN, modeling indirect effects at the heritable level only, using a subset of the neighbor positions.
[b]Differences (Δ) between models in AIC or BIC values were computed with respect to the more parsimonious model, that is: FN_2, when comparing FN_2 to FN_1, and thus $\Delta AIC_{(FN\_2,\ FN\_1)} = AIC_{(FN\_2)} - AIC_{(FN\_1)}$ and $\Delta BIC_{(FN\_2,\ FN\_1)} = BIC_{(FN\_2)} - BIC_{(FN\_1)}$; and RN, when comparing RN to FN_2, and thus $\Delta AIC_{(RN,\ FN\_2)} = AIC_{(RN)} - AIC_{(FN\_2)}$ and $\Delta BIC_{(RN,\ FN\_2)} = BIC_{(RN)} - BIC_{(FN\_2)}$.
[c]The neighbors kept in the RN model pertain to a reduced set of neighbor positions that were identified as having the greatest influence on the expression of IGEs (for more details on the comparison of the FN_2 and RN models, see Supplementary Note S4 in Supplementary Information).
[d]For either AIC or BIC values, there was a difference of nine fitted parameters when comparing the FN_1 and FN_2 models; for the RN/FN_2 model comparisons, the difference in the number of fitted parameters depended on the number of neighbor positions kept in the RN model (that is, the FN_2 and RN models differed in either five or six fitted parameters).
[e]An arcsine transformation was applied for the MLD data (see the Materials and methods section). To avoid convergence problems, which may occur when trait variances are very small, the transformed MLD data were then rescaled by multiplying the observations by 100. Thus, for MLD, the results tabulated above refer to the (arcsine) transformed and rescaled observations.

the extra model complexity. Under these circumstances, and as suggested by Kuha (2004), 'playing safe' and preferring the simpler, more parsimonious model is the best decision. Selection of an overly complex model is more likely when the true effect of a measured factor is relatively weak (Richards, 2008). This could be the case of MLD, as suggested by the estimate/standard error ratios of FA1 loadings estimated for indirect additive genetic effects being in general weaker for MLD than for DBH (see Supplementary Table S1 in Supplementary Information). Consequently, when compared with FN_1, modeling indirect effects at the additive genetic level only under FN_2 was preferred to FN_1 for these traits and ages.

In the sequential approach followed for comparing model RN to FN_2, the AIC and BIC preferred the same RN model for all the pairs of RN/FN_2 comparisons. For MLD and DBH at age 2 years, the RN model indicated by AIC included neighbor positions K_1 and K_2 only, but position K_4 was also included for DBH at ages 4 and 8 years. In all cases, the change in BIC from adding an extra neighbor position was >2, indicating empirical evidence against a more complex RN model (Kass and Raftery, 1995). Figure 2 illustrates the neighbors contributing most to IGEs for MLD and DBH at ages 2 and 4 years, respectively.

Modeling a combined indirect effect. Table 2 shows the genetic (co) variance parameters estimated by modeling IGEs as a combined effect, using either the full set (hereafter called FS) of eight immediate neighbors or a reduced set (hereafter called RS) comprising the most influential neighbors that were identified under model RN. Figure 3 and Supplementary Table S4 (Supplementary Information) present estimates over time for the total heritable variance [$\hat{Var}(TBV)$, where TBV denotes total breeding value] underlying potential response to selection, including the components of $\hat{Var}(TBV)$ due to direct and indirect genetic effects.

The $\hat{\sigma}^2_{a_d}$ estimate was found to be always highly significant ($P<0.001$), according to a one-tailed likelihood-ratio test; in addition, highly significant ($P<0.001$) outcomes were also always obtained by a two-tailed likelihood-ratio test of the overall significance of IGEs, and involving a joint test of both of the parameter estimates $\hat{\sigma}^2_{a_i}$ and $\hat{r}_{a_{di}}$. In general, no major changes were detected between the FS and RS neighborhoods for $\hat{\sigma}^2_{a_d}$, a trend that was also observed for $\hat{\sigma}^2_{a_d}/\hat{\sigma}^2_p$ ratios (that is, ordinary heritability; Figure 3 and Supplementary Table S4), as well as for the $\hat{r}_{a_{di}}$ estimates which are consistent with neighbor infection (MLD) and strong competition (DBH) (Table 2). However, while remaining virtually unchanged for MLD, the magnitude and significance (as indicated by the ratio of the parameter estimate relative to its standard error) of $\hat{\sigma}^2_{a_i}$ values for DBH increased under the RS analysis compared with those under the FS analysis, with the relative improvement in the magnitude of $\hat{\sigma}^2_{a_i}$ being accentuated with age (Table 2). These results were reflected in the ΔAIC obtained from comparing the RS and FS analyses for a given trait/age (not shown).

The contributions of IGEs to $\hat{Var}(TBV)$ differed between the FS and RS analyses for a given trait/age, reflecting a lower value under the RS neighborhood for the quantity $\overline{n_{row}f_{row}} + \overline{n_{col}f_{col}} + \overline{n_{diag}f_{diag}}$ in the equation used to calculate $\hat{Var}(TBV)$ (Costa e Silva and Kerr, 2013). For MLD under the RS, the reduction of the contribution of the indirect genetic variance, coupled with a lower positive contribution due to the direct–indirect genetic covariance, resulted in a decrease of $\hat{Var}(TBV)$ when compared with the FS (Figure 3). For DBH under the RS, and despite the increases observed in $\hat{\sigma}^2_{a_i}$ (Table 2), there was also a reduction at all ages of the contribution of the indirect genetic variance when compared with the FS; yet, the lower value for $\overline{n_{row}f_{row}} + \overline{n_{col}f_{col}} + \overline{n_{diag}f_{diag}}$ under the RS led to a less negative contribution due to the direct–indirect genetic covariance, which resulted in a net increase of $\hat{Var}(TBV)$ relative to the FS (Figure 3).

The contributions of IGEs to the total heritable variance also differed among traits/ages. When compared with $\hat{\sigma}^2_{a_d}$, IGEs increased $\hat{Var}(TBV)$ for MLD by 76 and 36% under the FS and RS, respectively, leading to corresponding $\hat{Var}(TBV)/\hat{\sigma}^2_p$ ratios of 0.75

Table 2 Additive genetic (co)variance components (± standard errors) estimated from a univariate model in which IGEs were modeled as a combined effect, using either full or reduced sets of neighbor positions[a,b,c,d,e,f]

Trait (age)	*All eight neighbor positions*			*Reduced set of neighbor positions*		
	$\hat{\sigma}^2_{a_d}$	$\hat{\sigma}^2_{a_i}$	$\hat{r}_{a_{di}}$	$\hat{\sigma}^2_{a_d}$	$\hat{\sigma}^2_{a_i}$	$\hat{r}_{a_{di}}$
MLD	78.18±13.81	1.63±0.65	0.82±0.13	82.96±14.45	1.50±0.62	0.83±0.13
(2 years)	(5.7)	(2.5)	(6.3)	(5.7)	(2.4)	(6.4)
DBH	91.27±16.18	6.08±1.50	−0.92±0.06	90.32±15.26	6.78±1.49	−0.90±0.06
(2 years)	(5.6)	(4.0)	(−15.3)	(5.9)	(4.6)	(−15.0)
DBH	218.12±29.60	32.27±5.18	−0.96±0.03	218.29±28.68	36.34±5.10	−0.95±0.03
(4 years)	(7.4)	(6.2)	(−32.0)	(7.6)	(7.1)	(−31.7)
DBH	708.05±72.62	116.74±14.13	−0.97±0.02	643.50±68.90	149.96±16.61	−0.95±0.03
(8 years)	(9.7)	(8.3)	(−48.5)	(9.3)	(9.0)	(−31.7)

Abbreviations: IGEs signifies indirect genetic effects; DBH and MLD denote stem diameter at breast-height and Mycosphearella leaf disease, respectively.
[a]The tabulated (co)variance parameter estimates refer to: $\hat{\sigma}^2_{a_d}$ = direct additive genetic variance; $\hat{\sigma}^2_{a_i}$ = indirect additive genetic variance; and $\hat{r}_{a_{di}}$ = direct–indirect additive genetic correlation. The ratio of the parameter estimate relative to its standard error is given in parenthesis.
[b]Modeling IGEs as a combined effect used either all eight immediate neighbors of a focal tree (Figure 2) or a subset of the neighbor positions that were found to contribute most to IGEs (that is, see 'Neighbors kept in RN' in Table 1).
[c]Results obtained from modeling IGEs as a combined effect by using all eight immediate neighbors were previously reported by Costa e Silva *et al.* (2013) for MLD at age 2 years, and DBH at ages 2 and 4 years. However, the results provided above for all neighbor positions differ slightly to those reported in Costa e Silva *et al.* (2013), as some parents have been subsequently re-allocated to the factorial to improve the number of families per parent and geographic focus of the parents in the diallel (see the Materials and methods section).
[d]For MLD, the parameter estimates refer to the (arcsine) transformed and rescaled observations (for more details, see footnote e of Table 1).
[e]A univariate model that ignored additive genetic terms involving IGEs was used as a base model to assess the statistical significance of the direct additive genetic variance via a one-tailed likelihood-ratio test (Stram and Lee, 1994). In this sense, a nested model constraining the estimate of the direct additive genetic variance to be zero was compared with the base model. For all traits and ages, the estimate of the direct additive genetic variance was found to be always highly significant ($P<0.001$).
[f]The complete univariate model that estimated both direct and indirect additive genetic (co)variances (providing the results tabulated above) was compared with a nested model that fitted only direct additive genetic effects, in order to carry out a joint test of significance for the variance and covariance parameter estimates involving IGEs. Using a two-tailed likelihood-ratio test, highly significant ($P<0.001$) results were detected for all traits and ages.

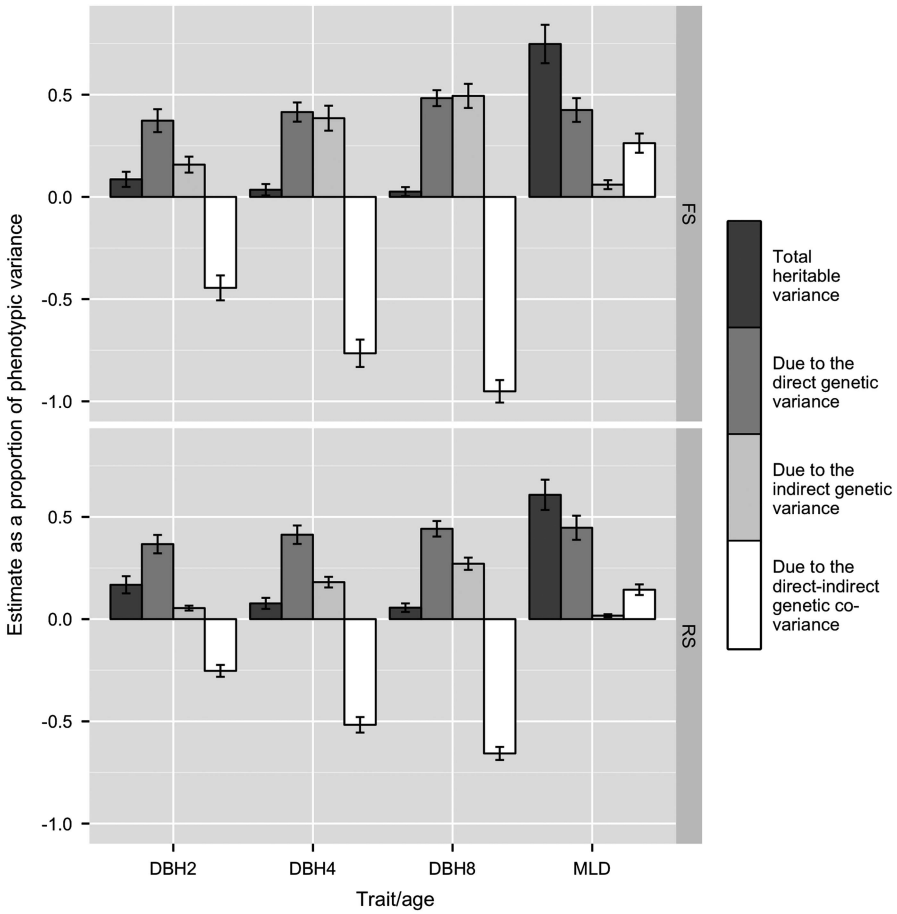

Figure 3 Relative contributions (that is, as a proportion of the phenotypic variance) to the total heritable variance due to the variances associated with direct and indirect genetic effects, and to their covariance, for breast-height stem diameter (DBH) growth at ages 2, 4 and 8 years, and for a damage due to a transient outbreak of Mycosphearella leaf disease (MLD) occurring at age 2 years, estimated using the full (FS) and reduced (RS) sets of neighbor positions. There is a marked contrast of the impact of IGEs on disease damage compared with growth: for MLD, the positive direct–indirect covariance (indicative of infection) significantly increased the total heritable variance in the population compared with the direct genetic variance; conversely, for DBH, the negative direct–indirect covariance (indicative of competition) resulted in a substantial decrease of the total heritable variance. For DBH, the relative magnitude of the indirect genetic variance and the direct–indirect genetic covariance increased more with age than the direct genetic variance did, but less between ages 4 and 8 years than between ages 2 and 4 years, leading to a stabilization of the impact of competitive interactions on the heritable variance at the later age. Further details on these results are provided in Supplementary Table S4 (Supplementary Information).

and 0.61, and thus were noticeably greater than the $\hat{\sigma}^2_{a_d}/\hat{\sigma}^2_p$ ratios of ≈ 0.4 (Supplementary Table S4). The IGEs reduced substantially $\hat{Var}(TBV)$ for DBH at all ages when compared with $\hat{\sigma}^2_{a_d}$ (Figure 3): the percentage decreases under the FS were 77, 92 and 95%, and those under the RS were 54, 81 and 87%, at ages 2, 4 and 8 years, respectively; this led to corresponding $\hat{Var}(TBV)/\hat{\sigma}^2_p$ ratios of 0.09, 0.04 and 0.03 under the FS, and 0.17, 0.08 and 0.06 under the RS (Supplementary Table S4). All of these $\hat{Var}(TBV)/\hat{\sigma}^2_p$ ratios were considerably lower than the $\hat{\sigma}^2_{a_d}/\hat{\sigma}^2_p$ ratios (varying from 0.37 to 0.48), indicating that the heritable competition expressed in DBH growth will substantially limit the potential for response to selection. Yet, these results over time suggest that the impact of competitive interactions among individuals on the heritable variance of DBH tended to stabilize at age 8 years (as also observed for $\hat{r}_{a_{di}}$ in Table 2). Indeed, although the component of $\hat{Var}(TBV)$ due to the direct–indirect genetic covariance was increasingly negative with age for DBH, the relative difference between ages 2 and 4 years was much greater than that between 4 and 8 years (Figure 3). These results clearly indicate a marked change in the competitive environment between ages 2 and 4 years, an interval usually associated with canopy closure.

Bivariate data analysis

On the basis of data analyses using a bivariate linear mixed model, estimates of genetic correlations—that is, correlations comprising the direct (a_d) and/or indirect (a_i) additive genetic effects, plus those involving *TBV*—are given in Table 3 for relationships between MLD measured at the age of infection (2 years) and post-infection DBH growth at ages 4 and 8 years, and in Table 4 for relationships between DBH measured at early (2 and 4 years) and late (8 years) ages. Preliminary analysis that used a simpler bivariate model fitting direct genetic effects only indicated a non-significant genetic correlation estimate (-0.03 ± 0.16) between MLD and DBH measured at age 2 years; no correlation is expected since DBH at this age effectively reflects growth before infection by Mycosphaerella. Thus, a more complex variance–covariance matrix (as defined in Equation [S_6]; see Supplementary Note S6) to estimate direct–indirect and indirect–indirect genetic correlations between these traits at age 2 years was not attempted.

The direction of the genetic correlations involving a_d and/or a_i effects was stable between MLD and post-infection DBH, but the magnitude and significance of the estimates decreased over time

Table 3 Genetic correlations (with standard errors in parenthesis) estimated between MLD measured at the age of infection (2 years) and post-infection DBH growth (ages 4 and 8 years)[a,b]

	DBH (4 years)			*DBH (8 years)*		
	a_d	a_i	TBV	a_d	a_i	TBV
MLD (2 years)						
a_d	−0.44 (±0.11)	0.42 (±0.10)	—	−0.31 (±0.11)	0.36 (±0.09)	—
a_i	−0.34 (±0.22)	0.41 (±0.24)	—	−0.07 (±0.24)	0.24 (±0.25)	—
TBV	—	—	−0.37 (±0.18)	—	—	0.01 (±0.21)

Abbreviations: IGEs signifies indirect genetic effects; DBH and MLD denote stem diameter at breast-height and Mycosphearella leaf disease, respectively.
[a]Additive genetic (co)variance components were estimated from a bivariate model in which IGEs were modeled as a combined effect, using a subset of the neighbor positions that were found to contribute most to IGEs (that is, see 'Neighbors kept in RN' in Table 1). The estimated (co)variances were used to derive genetic correlations between: the direct genetic effects (a_d) for the two traits; the a_d for one trait and the indirect genetic effect (a_i) for another, and *vice versa*; the a_i for the two traits; and the total breeding values (*TBV*) for the two traits.
[b]For MLD, the parameter estimates refer to the (arcsine) transformed and rescaled observations (for more details, see footnote e of Table 1).

Table 4 Genetic correlations (with standard errors in parenthesis) estimated between DBH growth measured at late (8 years) and early ages (2 and 4 years)[a]

	DBH (4 years)			*DBH (2 years)*		
	a_d	a_i	TBV	a_d	a_i	TBV
DBH (8 years)						
a_d	0.93 (±0.02)	−0.99 (±0.01)	—	0.79 (±0.05)	−0.94 (±0.03)	—
a_i	−0.94 (±0.02)	0.99 (±0.01)	—	–0.80 (±0.05)	0.95 (±0.03)	—
TBV	—	—	0.73 (±0.14)	—	—	0.60 (±0.15)

Abbreviations: IGEs, indirect genetic effects; DBH, stem diameter at breast-height.
[a]Additive genetic (co)variance components were estimated from a bivariate model in which IGEs were modeled as a combined effect, using a subset of the neighbor positions that were found to contribute most to IGEs (that is, see 'Neighbors kept in RN' in Table 1). The estimated (co)variances were used to derive genetic correlations between: the direct genetic effects (a_d) for the two traits; the a_d for one trait and the indirect genetic effect (a_i) for another, and *vice versa*; the a_i for the two traits; and the total breeding values (*TBV*) for the two traits.

(Table 3). Negative genetic correlation estimates indicated an adverse impact of MLD assessed at age 2 years on the a_d effects for later growth. This appeared mainly at the direct genetic level, as genotypes with higher a_d effects for damage by MLD were significantly associated with lower DBH in the focal tree ($\hat{r}_{a_d\_\mathrm{MLD},a_d\_\mathrm{DBH}} = -0.44 \pm 0.11$ and -0.31 ± 0.11 for DBH measured at ages 4 and 8 years, respectively) but did not reduce the growth of its neighbors. Rather, the a_d effects for MLD were significantly positively correlated with the a_i effects for DBH measured at ages 4 and 8 years ($\hat{r}_{a_d\_\mathrm{MLD},a_i\_\mathrm{DBH}} = 0.42 \pm 0.10$ and 0.36 ± 0.09). In addition, despite a highly positive $\hat{r}_{a_{di}}$ for MLD (Table 2), the estimated correlations between the a_i effects for MLD and the a_d effects for DBH did not appear to differ significantly from zero ($\hat{r}_{a_i\_\mathrm{MLD},a_d\_\mathrm{DBH}} = -0.34 \pm 0.22$ and -0.07 ± 0.24). These outcomes could be explained by the following: (1) a focal tree performing poorly for growth (a lower a_d effect for DBH) due to disease damage (a higher a_d effect for MLD) will compete less with its neighbors (a less negative, or even positive a_i effect for DBH), as indicated by the strong negative $\hat{r}_{a_{di}}$ (Table 2) estimate for DBH; and (2) this reduced competitive environment of the neighborhood as a whole could result in a favorable effect by countering any adverse impact that the increased risk of neighbor infection (a higher a_i effect for MLD, reflecting a strong positive $\hat{r}_{a_{di}}$ estimate; Table 2) would have on the DBH growth of neighboring trees. These putative explanations are also mirrored in the positive relationships between MLD and DBH for a_i effects, although the estimated genetic correlations did not appear to be significant particularly for DBH at age 8 years ($\hat{r}_{a_i\_\mathrm{MLD},a_i\_\mathrm{DBH}} = 0.24 \pm 0.25$). When the direct and indirect genetic effects were combined (as in Equations [S_9] and [S_10]; see Supplementary Note S7), a significant adverse overall association was obtained between MLD and post-infection DBH at age 4 years ($\hat{r}_{TBV\_\mathrm{MLD},TBV\_\mathrm{DBH}} = -0.37 \pm 0.18$), but was virtually zero for later growth ($\hat{r}_{TBV\_\mathrm{MLD},TBV\_\mathrm{DBH}} = 0.01 \pm 0.21$) (Table 3).

The results in Table 4 show that the direct–direct genetic correlations between DBH at ages 2 or 4 years and at age 8 years were positive and significant, although lower for age 2 (0.79 ± 0.05) than for age 4 (0.93 ± 0.02), a pattern also observed for the total breeding values (that is, 0.60 ± 0.15 versus 0.73 ± 0.14). The direct–indirect genetic correlations were all negative and significant among the early-late DBH relationships: the correlation between the a_d effects at age 2 years and the a_i effects at age 8 years (-0.80 ± 0.05) indicated that a genotype growing rapidly at an early stage will have (on average) a substantial negative heritable effect on the later growth of its neighbors; in addition, the correlation between the a_i effects at age 2 years and the a_d effects at age 8 years (-0.94 ± 0.03) is consistent with an early onset of competitive interactions for growth between a focal tree and its neighbors. For the a_i effects, the significant correlation estimates for DBH over time indicated that heritable competition effects were highly positively correlated between early and late growth stages.

DISCUSSION

A new approach to identify the most influential neighbors

A novel application using a factor analytic (FA) model enabled the modeling of indirect effects, at the non-heritable and/or heritable levels, as individual neighbor effects on a focal tree. For a given trait and age, a sequential approach comparing factor analytic models allowed the identification of a subset of neighbor positions with the greatest influence on the expression of IGEs. Although factor analytic models have been commonly applied for studying genotype by environment interaction (Smith *et al.*, 2001; Meyer, 2009), including forest trees (for example, Costa e Silva and Graudal, 2008; Cullis *et al.*,

2014), we are unaware of any studies where they have been used to study the interactions between neighbors at the genetic or non-genetic levels. However, structural equation modeling, which combines path and factor analyses, has been used to study phenotypic interactions underlying IGEs in plants (Wolf *et al.*, 2011) and animals (Santostefano *et al.*, 2016).

The application of the factor analytic model has the advantage that it allows for: (i) an initial testing of whether interaction effects can be partitioned into a genetic and non-genetic component; and (ii) directionality of the interaction effects to be empirically detected. In allowing for asymmetry, the factor analytic model enables the identification of the most influential neighbor positions, and these alone can subsequently be used to model a combined indirect effect. Our results also indicated that the relative importance of the contribution of each neighbor to IGEs was associated with the significance of the corresponding loading in the factor analytic model. When compared with all eight immediate neighbors, modeling IGEs as a combined effect of the most influential neighbors often resulted in increases in the magnitude and significance of the estimated indirect genetic variance, while estimates of narrow-sense heritability remained virtually unchanged. Forest genetics trials are generally smaller than that used in the present study, and IGEs may go unnoticed unless the most influential neighbors are identified. We have indeed observed this in other field trial analyses, in which a significant indirect genetic variance estimate has been detected after considering only a subset of neighbor positions (unpublished results). Thus, in forest trees, we suggest that quantitative genetic studies involving interactions among conspecifics commence with the identification of the neighbors contributing most to indirect effects (see Supplementary Figure S1 in Supplementary Information, and also the Discussion section in Costa e Silva and Kerr, 2013).

In the present study, the FA1 model was fitted to individual neighbor positions to explicitly investigate their influence on IGEs depending on directionality. If our interest had been focused mainly on distance, the FA1 model could have been fitted to distance categories (that is, in our case, three classes resulting from collapsing same-row, same-column or same-diagonal neighbors together). However, using a FA approach for the analysis of IGEs in animal systems will be limited by the fact that there is usually no positional basis for giving differential weights to individuals. Nevertheless, an application of the FA model in both farmed and wild animal systems could be possible where categories of interacting individuals can be identified, for example, based on the time the animals interact within a given pen/cage (Cantet and Cappa, 2008). In this sense, the length of time the animals share a pen could be used to collapse all pen mates onto a specified number of categories (for example, akin to collapsing neighboring trees onto distance classes), and then the FA model could be applied using these categories as a positional basis.

The most proximal trees are the most influential

The most influential neighbors varied with trait and age, but in all cases the same-row positions were identified as impacting most on IGEs. These trees were the spatially closest neighbors to the focal tree, and these results are consistent with the well-documented distance-related competition demonstrated in *E. globulus* (Soares and Tomé, 1999). Nevertheless, given that the same-row positions were also in the direction of cultivation and ripping, below-ground intra-row interactions may have been further facilitated by greater ease of root growth within rows due to less compacted soils (Misra and Gibbons, 1996). Although our results indicated that diagonal neighbors could be effectively ignored, the same-column (inter-row) neighbors were sometimes important depending on trait and age. Weaker competition effects of diagonal neighbors have also been reported for growth in eucalypt clones (Resende *et al.*, 2016) and Douglas-fir progenies (Cappa *et al.*, 2016). The present study found asymmetry in the effect of the same-column neighbor positions on the DBH growth of a focal tree. Specifically, only the southern same-column neighbor position (that is, K_4; Figure 2) was identified as contributing most to IGEs, and this did not become apparent until after canopy closure (age 4 years). In forest trees, asymmetric competition is expected with respect to size (Boyden *et al.*, 2008) and species (Canham *et al.*, 2004; Boyden *et al.*, 2005), but there is a paucity of reports of spatial asymmetry as we have observed. In the present case, the greater influence of the southern than the northern same-column position is not consistent with a shading effect, as in the southern hemisphere this position is the one which would be shaded by the focal tree and not the opposite. However, with *E. globulus* exhibiting a strong positive relationship between above-ground biomass and below-ground fine root surface and biomass (O'Grady *et al.*, 2006), *E. globulus* fine roots reported to start occupying inter-row planting space by 14 months of age (O'Grady *et al.*, 2005) and root systems of forest trees being often markedly asymmetric (Coutts *et al.*, 1999), there is a possibility that the asymmetry we have observed in DBH for the same-column positions after age 2 years reflects some form of below-ground root competition (Schenk, 2006). In this case, competition for water is the most likely below-ground factor in this Mediterranean climate, although nutrient competition alone or in combination with water stress cannot be dismissed (White *et al.*, 2009).

Age trends in genetic parameters estimated for DBH growth

Consistent with Costa e Silva *et al.* (2013), our results suggest that predictions of response to selection based on quantitative genetic models ignoring IGEs may be overestimated for growth and underestimated for disease susceptibility. This conclusion holds regardless of whether modeling IGEs as a combined effect was undertaken with the full neighborhood or with just the most influential neighbors. In particular, the significant variance due to IGEs and strong negative correlation between direct and indirect genetic effects observed in the latest 8-year DBH measurement were consistent with earlier-age estimates, and they demonstrate strong genetic-based competitive interactions for growth. Other studies with forest trees have also reported such heritable competition for diameter growth (Resende *et al.*, 2005; Cappa and Cantet, 2008; Brotherstone *et al.*, 2011; Cappa *et al.*, 2015, 2016). Heritable competition is of particular concern in selection experiments, as strong competitors will appear better and poor competitors worse than they would in a production environment where genotypes are more similar in their competitive ability (Muir, 2005; Bijma *et al.*, 2007; Muir *et al.*, 2013). The competition observed among neighbor trees is akin to the negative effects of social interactions in animals (Ellen *et al.*, 2014; Wilson, 2014), demonstrating the constraints imposed by the 'social environment' on response to selection. High negative correlations between direct and indirect genetic effects were reported for growth in Japanese quail (Muir, 2005) and for survival time in crossbreed laying hens (Peeters *et al.*, 2012). Strong negative social interactions were also observed in deer mice (Wilson *et al.*, 2009), red deer (Wilson *et al.*, 2011) and fighting cows (Sartori and Mantovani, 2013).

Competition is positively related to neighbor tree size in *E. globulus* (Soares and Tomé, 1999), and it is expected to increase with age. Although the results for DBH showed a marked impact of competitive interactions on the heritable variance, this tended to stabilize after

canopy closure as indicated by diminishing rates of change in genetic parameters associated with IGEs. Nevertheless, the total heritable variance for DBH was still declining between ages 4 and 8 years due to the increasingly negative direct–indirect genetic covariance, although both indirect and direct genetic variances increased with stand development. This dynamic interplay between increasing expression of genetic effects with age being countered by competition has analogies in classical heritability studies of *E. globulus* (Stackpole *et al.*, 2010).

Genetic correlations

A multivariate approach is important to allow the identification of the interacting phenotypes responsible for the IGEs affecting the expression of a given trait (Wolf *et al.*, 2011; Bailey and Hoskins, 2014). For example, in a QTL study where the same (standard) neighbor plant genotype was interacting with different focal genotypes from a set of *Arabidopsis* recombinant inbred lines, Mutic and Wolf (2007) and Wolf *et al.* (2011) showed that not only did the QTL have pleiotropic direct effects on multiple traits in the focal plant phenotype, but also 'pleiotropic indirect' effects on traits expressed in neighboring individuals. These effects were reported for size and developmental traits. Mutic and Wolf (2007) recognized both non-reciprocal and reciprocal pleiotropic interactions, to differentiate cases where, respectively: (i) the expression of a trait in an individual is influenced by another trait in another individual, but the second trait is not affected by the interaction; and (ii) a trait expression in an individual is affected by a second trait in another individual and *vice versa* (see also Moore *et al.*, 1997). Wolf *et al.* (2011) further differentiated cases of identified and unidentified pleiotropy, where there is and there is not a functional/causal connection between the direct genetic effect on one trait and the IGE on a different trait, respectively. In the latter case, correlations between a direct genetic effect on one trait and the IGE on another trait can arise through pleiotropic direct genetic effects involving an unmeasured trait, which provides the mechanistic pathway for the IGE. Bailey and Hoskins (2014) similarly identified such interactions as cryptic IGEs in a study of *Drosophila melanogaster*, where the direct and indirect genetic effects for the same trait (male leg-tapping) were uncorrelated.

In the present study, a greater complexity to neighbor interactions was revealed by the bivariate models involving disease damage and diameter growth at various ages. For each trait, there were significant correlations between direct and indirect genetic effects, with IGEs reflecting an increased probability of neighbor infection and strong competition (consistent with Costa e Silva *et al.*, 2013). Although the high direct–indirect correlation observed for MLD damage (that is, $\hat{r}_{a_{di}} \approx 0.8$; Table 2) suggests that these IGEs simply reflect variation in neighbor disease exposure arising from genetic variation in focal tree susceptibility, the possibility of genetic variation in infectivity *per se* cannot be dismissed (Lipschutz-Powell *et al.*, 2012; Anche *et al.*, 2014). At the time of infection (age 2 years), no significant direct genetic correlation was observed between MLD damage and DBH growth. However, later-age growth measurements revealed a significant adverse, direct genetic correlation between MLD damage and subsequent growth. For *E. globulus*, such genetic signatures of MLD damage on subsequent growth have been reported previously (Milgate *et al.*, 2005), and are no doubt a pleiotropic direct effect of QTL affecting disease susceptibility (Freeman *et al.*, 2008). While the initial MLD infection may favor faster growing plants in some cases (Milgate *et al.*, 2005), this was not evident in the present study, and all evidence suggests that the direct, post-infection genetic correlations between these two traits reflect an adverse, non-reciprocal pleiotropic effect of disease damage on later-age growth. This functional conclusion follows from the well-documented adverse effects of pests and diseases on the growth of plantation-grown eucalypts (Eyles *et al.*, 2013). MLD infection can lead to varying levels of premature leaf defoliation in *E. globulus* (Carnigie and Ades, 2003; Pinkard and Mohammed, 2006). Diameter growth of *E. globulus* is reduced following canopy defoliation (Carnegie and Ades, 2003; Quentin *et al.*, 2011). In addition, leaves retained after MLD infection exhibit reduced photosynthetic capacity (Pinkard and Mohammed, 2006).

Despite adverse pleiotropic effects of disease damage on productivity at the direct genetic level, the IGEs arising from disease damage were not associated with a reduction in the growth of neighbors. Rather, increased disease damage on a focal tree (direct genetic effect) was associated with increased neighbor growth (indirect genetic effect) at a population level, despite the higher risk of neighbor infection. The reduced IGEs due to competition from slower-growing focal trees damaged by MLD thus appear to have over-ridden any adverse effects on growth of the increased risk of disease infection in the neighbors. This countering effect of IGEs for growth is sufficiently strong to result by age 8 years in: (i) a positive but non-significant correlation between the IGEs of MLD damage and growth; and (ii) a negligible correlation between the total breeding values of MLD damage and growth. The transient effect of the MLD damage on growth observed for the total breeding values was not evident for the direct breeding values, and no doubt will depend on the level of infection and strength of the adverse direct genetic effects of disease damage on growth. For example, a more enduring impact may be expected in outbreaks such as those reported by Milgate *et al.* (2005), where the average level of disease infection was higher (that is, 34% leaf area damaged compared with 23% observed in the present study) and the adverse direct genetic correlation with growth was stronger (that is, -0.77 versus our estimate of -0.44 at age 4 years).

Regardless of the dynamics associated with the interaction of IGEs for disease damage and growth, for growth itself the correlations involving indirect genetic effects remained relatively stable across ages. At the phenotypic level, the onset of competition in *E. globulus* plantings has been reported to occur between 21 and 31 months, depending on factors such as spacing and site productivity, with a shift from symmetric to asymmetric competition, as smaller trees become suppressed with age (Soares and Tomé, 1996). As indicated from univariate analyses of DBH, the increase in the relative importance of IGEs observed between ages 2 and 4 years, and attributed to increasing competition associated with canopy closure, appeared to stabilize at 8 years. In addition, the bivariate analyses of DBH across ages revealed that IGEs established at age 2 years remained stable through stand development. This is indicated by the age-to-age correlations between the IGEs not differing significantly from one, and even being higher than the genetic correlations between the direct genetic effects. Although strong age-to-age genetic correlations for direct genetic effects on growth are well established for forest trees (Stackpole *et al.*, 2010), this is the first report for IGEs. Our declining age-to-age correlations for direct genetic effects and total breeding values are consistent with the tendency generally observed with increasing age difference. However, the absence of such an obvious decline for correlations involving IGEs is noteworthy, and may reflect either a time lag in their diminution or an inherent stability in competitive effects. Such stability may arise from an inherent greater susceptibility of smaller trees to competition reducing growth (Boyden *et al.*, 2008), thus buffering changes in genetic-based competition with age.

Implications for wild populations

Although IGEs are clearly an important part of a tree's environment in plantations, the extent to which the observed IGEs impact the eco-evolutionary dynamics of wild populations can only be inferred (Costa e Silva *et al.*, 2013). As with heritability (Andrew *et al.*, 2005), studies of IGEs in wild populations are rare (Wilson *et al.*, 2011), but increasingly possible using large-scale pedigree reconstruction with molecular markers. Understanding the mechanisms, including interaction feedbacks, by which IGEs manifest (Trubenová *et al.*, 2015) and the demographic dynamics of IGEs (Wilson *et al.*, 2011) will be important. While some forest tree species grow in pure stands and regenerate *en masse*, creating even-aged monospecific cohorts similar to our planted population, in others recruitment is more continuous (Ashton, 2000). In these cases, the strongest interactions are likely across cohorts with pre-established, often related, phenotypes. The extent to which indirect genetic effects at the intraspecific level (IGEs) constitute a significant component of the biotic environment in the wild must also be assessed against the multitude of interspecific interactions (IIGEs) occurring at diverse trophic levels, from microbes to predators (Whitham *et al.*, 2008). Such studies are basic for our understanding of the role of indirect genetic effects in shaping natural patterns of genetic diversity and response to environmental change (Bailey *et al.*, 2014).

DATA ARCHIVING

The trials and germplasm studied are being used for commercial tree-breeding purposes. The raw data used for this study are subject to pre-existing agreements and cannot be made public. The raw data have been archived on the long-term data management system of the Southern Tree Breeding Association Inc. (STBA; Mount Gambier, Australia). The authors should be contacted if there is interest in use of these data for collaborative research purposes.

CONFLICT OF INTEREST

The authors declare no conflict of interest.

ACKNOWLEDGEMENTS

The financial support given to João Costa e Silva by *Fundação para a Ciência e a Tecnologia* (Lisboa, Portugal), through the *Programa Operacional Potencial Humano* and the European Social Fund, is gratefully acknowledged. The trial was established by the Southern Tree Breeding Association Inc. (STBA) on a site provided by WAPRES. Data collection were coordinated by David Pilbeam (STBA), and supported by Australian Research Council Grants (LP0884001 and LP140100506), seedEnergy Pty Ltd, STBA and CRC for Forestry. We thank David Pilbeam and Greg Dutkowski for their discussion over the course of this study.

Akaike H (1974). A new look at the statistical model identification. *IEEE Trans Autom Control* **19**: 716–723.

Anche MT, de Jong MCM, Bijma P (2014). On the definition and utilization of heritable variation among hosts in reproduction ratio R-0 for infectious diseases. *Heredity* **113**: 364–374.

Andrew RL, Peakall R, Wallis IR, Wood JT, Knight EJ, Foley WJ (2005). Marker-based quantitative genetics in the wild?: the heritability and genetic correlation of chemical defenses in *Eucalyptus*. *Genetics* **171**: 1989–1998.

Ashton DH (2000). Ecology of eucalypt regeneration. In: Keane PJ, Kile GA, Podger FD, Brown BN (eds). *Diseases and Pathogens of Eucalypts*. CSIRO Publishing: Collingwood, pp 35–46.

Bailey JK, Genung MA, Ware I, Gorman C, Van Nuland ME, Long H *et al.* (2014). Indirect genetic effects: an evolutionary mechanism linking feedbacks, genotypic diversity and coadaptation in a climate change context. *Funct Ecol* **28**: 87–95.

Bailey NW, Hoskins JL (2014). Detecting cryptic indirect genetic effects. *Evolution* **68**: 1871–1882.

Bijma P (2011). A general definition of the heritable variation that determines the potential of a population to respond to selection. *Genetics* **189**: 1347–1359.

Bijma P (2014). The quantitative genetics of indirect genetic effects: a selective review of modelling issues. *Heredity* **112**: 61–69.

Bijma P, Muir WA, Van Arendonk JAM (2007). Multilevel selection 1: quantitative genetics of inheritance and response to selection. *Genetics* **175**: 277–288.

Boyden S, Binkley D, Senock R (2005). Competition and facilitation between *Eucalyptus* and nitrogen-fixing Falcataria in relation to soil fertility. *Ecology* **86**: 992–1001.

Boyden S, Binkley D, Stape JL (2008). Competition among *Eucalyptus* trees depends on genetic variation and resource supply. *Ecology* **89**: 2850–2859.

Brotherstone S, White IMS, Sykes R, Thompson R, Connolly T, Lee S *et al.* (2011). Competition effects in a young Sitka spruce (*Picea sitchensis*, Bong. Carr) clonal trial. *Silvae Genet* **60**: 149–155.

Burnham KP, Anderson DR (2002). *Model Selection and Multimodel Inference: A Practical Information-Theoretic Approach*. Springer-Verlag: New York, NY, USA.

Camerlink I, Ursinus WW, Bijma P, Kemp B, Bolhuis JE (2015). Indirect genetic effects for growth rate in domestic pigs alter aggressive and manipulative biting behaviour. *Behav Genet* **45**: 117–126.

Canham CD, LePage PT, Coates KD (2004). A neighborhood analysis of canopy tree competition: effects of shading versus crowding. *Can J Forest Res* **34**: 778–787.

Cantet RJC, Cappa EP (2008). On identifiability of (co)variance components in animal models with competition effects. *J Anim Breed Genet* **125**: 371–381.

Cappa EP, Cantet RJC (2008). Direct and competition additive effects in tree breeding: Bayesian estimation from an individual tree mixed model. *Silvae Genet* **57**: 45–56.

Cappa EP, Muñoz F, Sanchez L, Cantet RJC (2015). A novel individual-tree mixed model to account for competition and environmental heterogeneity: a Bayesian approach. *Tree Genet Genomes* **11**: 120.

Cappa EP, Stoehr MU, Xie CY, Yanchuk AD (2016). Identification and joint modelling of competition effects and environmental heterogeneity in three Douglas-fir (*Pseudotsuga menziesii* var. *menziesii*) trials. *Tree Genet Genomes* **12**: 102.

Carnegie AJ, Ades PK (2003). *Mycosphaerella* leaf disease reduces growth of plantation-grown *Eucalyptus globulus*. *Aust For* **66**: 113–119.

Costa e Silva J, Graudal L (2008). Evaluation of an international series of *Pinus kesiya* provenance trials for growth and wood quality traits. *Forest Ecol Manag* **255**: 3477–3488.

Costa e Silva J, Kerr RJ (2013). Accounting for competition in genetic analysis, with particular emphasis on forest genetic trials. *Tree Genet Genomes* **9**: 1–17.

Costa e Silva J, Potts BM, Bijma P, Kerr RJ, Pilbeam DJ (2013). Genetic control of interactions amongst individuals: Contrasting outcomes of indirect genetic effects arising from neighbour disease infection and competition in a forest tree. *New Phytol* **197**: 631–641.

Coutts MP, Nielsen CCN, Nicoll BC (1999). The development of symmetry, rigidity and anchorage in the structural root system of conifers. *Plant Soil* **217**: 1–15.

Cullis BR, Jefferson P, Thompson R, Smith AB (2014). Factor analytic and reduced animal models for the investigation of additive genotype-by-environment interaction in out-crossing plant species with application to a *Pinus radiata* breeding programme. *Theor Appl Genet* **127**: 2193–2210.

Ellen ED, Bas Rodenburg T, Albers GAA, Bolhuis JE, Camerlink I, Duijvesteijn N *et al.* (2014). The prospects of selection for social genetic effects to improve welfare and productivity in livestock. *Front Genet* **5**: 377.

Eyles A, Barry KM, Quentin A, Pinkard EA (2013). Impact of defoliation in temperate eucalypt plantations: Physiological perspectives and management implications. *Forest Ecol Manag* **304**: 49–64.

Freeman JS, Potts BM, Vaillancourt RE (2008). Few Mendelian genes underlie the quantitative response of a forest tree, *Eucalyptus globulus,* to a natural fungal epidemic. *Genetics* **178**: 563–571.

Gilmour AR, Thompson R, Cullis BR (1995). Average information REML: an efficient algorithm for variance parameter estimation in linear mixed models. *Biometrics* **51**: 1440–1450.

Gilmour AR, Gogel BJ, Cullis BR, Welham SJ, Thompson R (2015). *ASReml User Guide Release 4.1*. VSN International Ltd: Hemel Hempstead, HP1 1ES, UK.

Griffing B (1967). Selection in reference to biological groups. I. Individual and group selection applied to populations of unordered groups. *Aust J Biol Sci* **20**: 127–139.

John JA, Williams ER (1995). *Cyclic and Computer Generated Designs*. Chapman and Hall: London, UK.

Kass RE, Raftery AE (1995). Bayes factors. *J Am Stat Assoc* **90**: 773–795.

Kuha J (2004). AIC and BIC: comparisons of assumptions and performance. *Soc Methods Res* **33**: 188–229.

Lipschutz-Powell D, Woolliams JA, Bijma P, Doeschl-Wilson AB (2012). Indirect genetic effects and the spread of infectious disease: are we capturing the full heritable variation underlying disease prevalence? *PLoS ONE* **7**: e39551.

Lynch M, Walsh B (1998). *Genetics and Analysis of Quantitative Traits*. Sinauer Associates, Sunderland: MA, USA.

McGlothlin JW, Brodie ED III (2009). How to measure indirect genetic effects: the congruence of trait-based and variance-partitioning approaches. *Evolution* **63**: 1785–1795.

McGlothlin JW, Moore AJ, Wolf JB, Brodie ED III (2010). Interacting phenotypes and the evolutionary process. III. Social Evolution. *Evolution* **64**: 2558–2574.

Meyer K (2009). Factor-analytic models for genotype x environment type problems and structured covariance matrices. *Genet Sel Evol* **41**: 21.

Milgate AW, Potts BM, Joyce K, Mohammed C, Vaillancourt RE (2005). Genetic variation in *Eucalyptus globulus* for susceptibility to *Mycosphaerella nubilosa* and its association with tree growth. *Australas Plant Pathol* **34**: 11–18.

Misra RK, Gibbons AK (1996). Growth and morphology of eucalypt seedling-roots, in relation to soil strength arising from compaction. *Plant Soil* **182**: 1–11.
Moorad JA, Nussey DH (2016). Evolution of maternal effect senescence. *Proc Natl Acad Sci USA* **113**: 362–367.
Moore AJ, Brodie ED III, Wolf JB (1997). Interacting phenotypes and the evolutionary process. 1. Direct and indirect genetic effects of social interactions. *Evolution* **51**: 1352–1362.
Muir WM (2005). Incorporation of competitive effects in forest tree or animal breeding programs. *Genetics* **170**: 1247–1259.
Muir WM, Bijma P, Schinckel A (2013). Multilevel selection with kin and non-kin groups, experimental results with Japanese quail (*Coturnix japonica*). *Evolution* **67**: 1598–1606.
Mutic JJ, Wolf JB (2007). Indirect genetic effects from ecological interactions in *Arabidopsis thaliana*. *Mol Ecol* **16**: 2371–2381.
O'Grady AP, Worledge D, Battaglia M (2005). Temporal and spatial changes in fine root distributions in a young *Eucalyptus globulus* stand in southern Tasmania. *Forest Ecol Manag* **214**: 373–383.
O'Grady AP, Worledge D, Battaglia M (2006). Above- and below-ground relationships, with particular reference to fine roots, in a young *Eucalyptus globulus* (Labill.) stand in southern Tasmania. *Trees* **20**: 531–538.
Peeters K, Eppink T, Ellen ED, Visscher J, Bijma P (2012). Indirect genetic effects for survival in domestic chicken (*Gallus gallus*) are magnified in crossbred genotypes and show a parent-of-origin effect. *Genetics* **192**: 705–713.
Pinkard EA, Mohammed CL (2006). Photosynthesis of *Eucalyptus globulus* with *Mycosphaerella* leaf disease. *New Phytol* **170**: 119–127.
Quentin AG, Beadle CL, O'Grady AP, Pinkard EA (2011). Effects of partial defoliation on closed canopy *Eucalyptus globulus* Labilladiere: Growth, biomass allocation and carbohydrates. *Forest Ecol Manag* **261**: 695–702.
Resende MDV, Stringer JK, Cullis BR, Thompson R (2005). Joint modelling of competition and spatial variability in forest field trials. *Rev Mat Estat* **23**: 7–22.
Resende RT, Marcatti GE, Pinto DS, Takahashi EK, Cruz CD, Resende MDV (2016). Intragenotypic competition of *Eucalyptus* clones generated by environmental heterogeneity can optimize productivity in forest stands. *Forest Ecol Manag* **380**: 50–58.
Richards SA (2008). Dealing with overdispersed count data in applied ecology. *J Appl Ecol* **45**: 218–227.
Santostefano F, Wilson AJ, Araya-Ajoy YG, Dingemanse NJ (2016). Interacting with the enemy: indirect effects of personality on conspecific aggression in crickets. *Behav Ecol* **27**: 1235–1246.
Sartori C, Mantovani R (2013). Indirect genetic effects and the genetic bases of social dominance: evidence from cattle. *Heredity* **110**: 3–9.
Schenk HJ (2006). Root competition: beyond resource depletion. *J Ecol* **94**: 725–739.
Schwarz G (1978). Estimating the dimension of a model. *Ann Stat* **6**: 461–464.
Shuster SM, Lonsdorf EV, Wimp GM, Bailey JK, Whitham TG (2006). Community heritability measures the evolutionary consequences of indirect genetic effects on community structure. *Evolution* **60**: 991–1003.
Soares P, Tomé M (1996). Changes in eucalypt plantations structure, variability and relative growth rate pattern under different intraspecific competition gradients. In: Skovsgaard JP, Johannsen VK (eds). *Modelling Regeneration Success and Early Growth of Forest Stands*. Proceedings from the IUFRO Conference (Copenhagen, 10–13 June 1996). Danish Forest and Landscape Research Institute: Hørsholm, pp 270–284.
Soares P, Tomé M (1999). Distance-dependent competition measures for *Eucalyptus* plantations in Portugal. *Ann Forest Sci* **56**: 307–319.
Smith AB, Cullis BR, Thompson R (2001). Analyzing variety by environment data using multiplicative mixed models and adjustments for spatial field trend. *Biometrics* **57**: 1138–1147.
Stackpole DJ, Vaillancourt RE, Aguigar M, Potts BM (2010). Age trends in genetic parameters for growth and wood density in *Eucalyptus globulus*. *Tree Genet Genomes* **6**: 179–193.
Stram DO, Lee JW (1994). Variance components testing in the longitudinal mixed effects model. *Biometrics* **50**: 1171–1177.
Trubenová B, Novak S, Hager R (2015). Indirect genetic effects and the dynamics of social interactions. *PLoS ONE* **10**: e0126907.
White DA, Crombie DS, Kinal J, Battaglia M, McGrath JF, Mendham DS *et al.* (2009). Managing productivity and drought risk in *Eucalyptus globulus* plantations in south-western Australia. *Forest Ecol Manag* **259**: 33–44.
Whitham TG, DiFazio SP, Schweitzer JA, Shuster SM, Allan GJ, Bailey JK *et al.* (2008). Extending genomics to natural communities and ecosystems. *Science* **320**: 492–495.
Wilson AJ (2014). Competition as a source of constraint on life history evolution in natural populations. *Heredity* **112**: 70–78.
Wilson AJ, Gelin U, Perron M-C, Réale D (2009). Indirect genetic effects and the evolution of aggression in a vertebrate system. *Proc R Soc B Biol Sci* **276**: 533–541.
Wilson AJ, Morrissey MB, Adams MJ, Walling CA, Guinness FE, Pemberton JM *et al.* (2011). Indirect genetics effects and evolutionary constraint: an analysis of social dominance in red deer, *Cervus elaphus*. *J Evol Biol* **24**: 772–783.
Wolf JB, Brodie ED III, Cheverud JM, Moore AJ, Wade MJ (1998). Evolutionary consequences of indirect genetic effects. *Trends Ecol Evol* **13**: 64–69.
Wolf JB, Mutic JJ, Kover PX (2011). Functional genetics of intraspecific ecological interactions in *Arabidopsis thaliana*. *Philos Trans R Soc B Biol Sci* **366**: 1358–1367.

Supplementary Information accompanies this paper on Heredity website (http://www.nature.com/hdy)